SIMULTANEOUS EVAPORATION OF TWO ADJACENT VOLATILE DROPS

IZUMI TANIGUCHI, TAKAHIRO KAWAHARA AND KOICHI ASANO
Department of Chemical Engineering,
Tokyo Institute of Technology, Tokyo 152

Key Words: Atomization, Mass Transfer, Evaporation, Two Drops, High Mass Flux, Transfer Number

Measurements were made of the effect of interaction between two drops on the simultaneous evaporation of two coaxially arranged water and hexane drops for Re_{PA}=64–230, Sc=0.59–1.57, D_B/D_A=0.54–1.58, L/D_A=0.98–11.04 and B_M=0.02–0.64.

The observed diffusion fluxes for water drops were compared with the previous numerical solutions. A systematic deviation from the previous numerical solution under low mass flux conditions was observed for hexane drops. New correlations for the diffusion fluxes of two adjacent drops were proposed by considering the effect of the interaction between two drops, of high mass flux and of variable properties.

Introduction

Simultaneous evaporation of two adjacent liquid drops is important in studies of spray drying, quenching of hot gas or combustion of liquid fuel. Although in the past decades some theoretical or experimental approaches[1,3,6,9,10,13,14] have been made to the effect of interaction between two adjacent drops, most of them are concerned with those under low mass flux conditions or those for quiescent fluid. Recently Miura *et al.*[6] made an experimental approach to heat and mass transfer of two adjacent water drops for the intermediate Reynolds number range. Rex *et al.*[9] made an experimental approach to the burning of two adjacent fuel drops in quiescent fluid, but their results were limited to those under low mass flux conditions or at low Reynolds number. The present authors made theoretical and experimental approaches[2,11,12] to this problem under low mass flux conditions.

The purpose of the present work is to make an experimental approach to the effect of interaction

Received July 18, 1989. Correspondence concerning this article should be addressed to K. Asano.

between two drops under high mass flux conditions and for intermediate Reynolds number ranges.

1. Experimental Apparatus and Procedures

1.1 Experimental apparatus

Figure 1 shows a schematic diagram of the experimental apparatus. The test section was a rectangular brass duct of 60 × 40 mm cross section and 520 mm length, with a large side-view window. In the middle of the test section, two stainless steel tubes for liquid supply were mounted and were connected to microfeeder-operated hypodermic syringes. A 0.05 mm-outer diameter Chromel-Alumel thermocouple was mounted by a three-dimensional fine-adjustment traversing mechanism for measurements of drop temperature.

Air was supplied to the test section by a blower through a silica gel-packed dehumidifier, a 1 kW electric heater and a convergent nozzle packed with 5 mm- and 10 mm-outer diameter brass tube calming grids.

1.2 Measurement

1) Rates of evaporation Liquid to evaporating pendant drops was supplied by two calibrated variable-flow-rate microfeeders. Rates of evaporation of pendant drops were taken equal to equilibrium flow rates of liquid supplied by microfeeders, of which the flow rates were so adjusted that the diameter of the drop did not change appreciably for a given time interval.

2) Distance between two drops and drop diameters The distance between the centers of two coaxially arranged drops were measured by a cathetometer with an accuracy of 1/100 mm. Diameters of pendant drops were also measured by the cathetometer, from which surface areas of the drops were calculated by assuming that the shape of the drop was axially symmetrical.[5]

3) Surface temperatures and concentrations of evaporating drops The drop temperatures were measured by a 0.05 mm-outer diameter Chromel-Alumel thermocouple mounted on a three-dimensional fine-adjustment traversing mechanism, from which the surface temperatures of evaporating drops were estimated by assuming that the temperature distribution inside the drop is uniform.[5] Surface concentrations of the evaporating drops were estimated from saturated vapor pressures of the pure liquid at surface temperatures.

1.3 Ranges of variables and physical properties

Evaporation runs were made for water-air system and hexane-air system at atmospheric pressure. Ranges of variables are shown in **Table 1**.

Physical properties were evaluated at their surface conditions. Vapor pressures of the liquid were estimated by Antoine's equation. Binary diffusion coefficients and viscosities of pure vapors were estimated by Hirschfelder's method,[8] and thermal conductivities of pure vapors by Eucken's method.[8] Viscosities and thermal conductivities of mixed vapors were estimated by Wilke's method.[8]

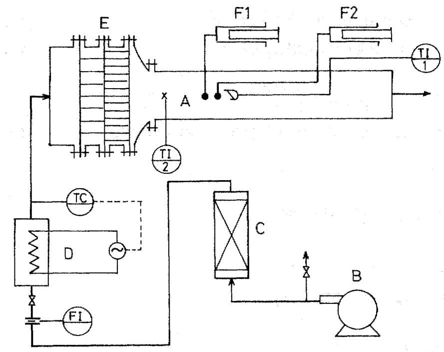

A : Test section
B : Blower
C : Silica gel dehumidifier
D : Heater
E : Divergent convergent nozzle with calming grid
F1, 2: Microfeeder
FI : Orifice flow meter
TC : Temperature controller
TI : Thermocouple for 1: liquid drop 2: bulk flow

Fig. 1. Schematic diagram of experimental apparatus

Table 1. Ranges of experimental variables

System		Water-air	Hexane-air
D_A	[mm]	1.53–2.89	1.69–2.51
D_B	[mm]	1.54–3.02	1.61–2.70
L	[mm]	1.96–19.61	2.19–6.99
T_∞	[K]	323–365	301–342
U_∞	[m/s]	0.45–1.50	0.59–0.61
Re_{PA}	[—]	64–230	122–219
Sc	[—]	0.59	1.57–1.10
B_M	[—]	0.02–0.05	0.25–0.64
L/D_A	[—]	0.98–11.04	1.05–3.45
D_B/D_A	[—]	0.54–1.58	0.81–1.15

2. Experimental Results

2.1 Evaporation of two coaxially arranged water drops

In order to confirm the validity of the present method, measurements of the rates of evaporation of single water drop were carried out to show good agreement with the Ranz-Marshall's correlation within less than 10%.

Figure 2 shows experimental results for evaporation of coaxially arranged water drops into dry air under low mass flux conditions. The dimensionless diffusion fluxes of the rear drops for various Reynolds numbers ranging from 70 to 200 but at nearly the same diameter ratios ($D_B/D_A = 1$) were plotted against dimensionless distances between two drops. The $[Sh(1-\omega_S)]_0$ values in the ordinate are those for a single sphere calculated by Ranz-Marshall's correlation[7]:

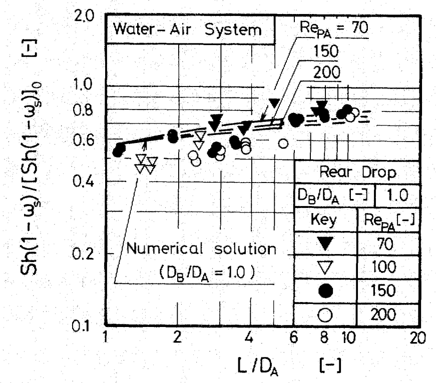

Fig. 2. Diffusion fluxes of rear drops at intermediate Reynolds number

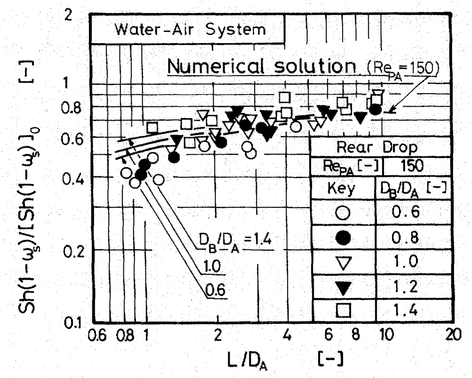

Fig. 3. Effect of diameter ratio on diffusion fluxes of rear drops

$$[Sh(1-\omega_S)]_0 = 2 + 0.6 \cdot Re_P^{1/2} \cdot Sc^{1/3} \qquad (1)$$

The solid line in the figure represents the numerical correlation proposed in our previous papers[2,12]:

$$\frac{Sh(1-\omega_S)}{[Sh(1-\omega_S)]_0} = f_B = \frac{1}{1+0.77\cdot(D_B/D_A)^{-0.21}\cdot(L/D_A)^{-1.38\cdot Re_{PA}^{-0.26}}} \qquad (2)$$

The observed diffusion fluxes showed fairly good agreement with the numerical correlation. This fact may indicate that the numerical correlation developed for low Reynolds number ranges ($1 \leqq Re_{PA} \leqq 30$) can also be applied to intermediate Reynolds number ranges.

Figure 3 shows the effect of the distances between two drops on the diffusion fluxes of the rear drops. The solid lines in the figure are the predictions by Eq. (2) for $D_B/D_A = 0.6$, 1.0 and 1.4, respectively. Although some scattering of the data is observed at low values of L/D_A, fairly good agreement between the data and the correlation is observed.

Figure 4 shows a comparison of the observed data for the diffusion fluxes of the rear drops with the previous numerical correlation under low mass flux conditions (Eq. (2)). Good agreement is observed between the data and the correlation.

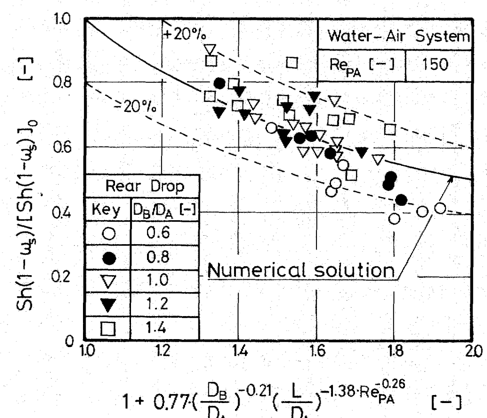

Fig. 4. Diffusion fluxes of rear drops under low mass flux conditions; comparison with numerical results

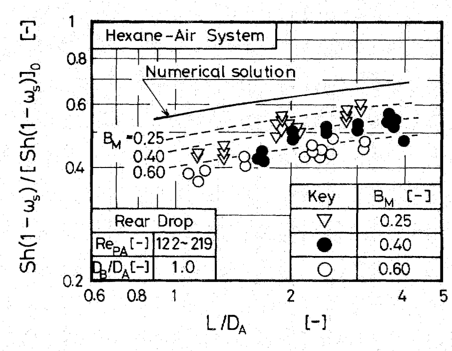

Fig. 5. Diffusion fluxes of rear drop under high mass flux conditions

2.2 Evaporation of two coaxially arranged hexane drops

Figure 5 shows the diffusion fluxes of the rear drops for evaporation of coaxially arranged hexane drops into dry air under high mass flux conditions. B_M in the figure is the transfer number for mass transfer, defined by:

$$B_M = (\omega_S - \omega_\infty)/(1-\omega_S) \qquad (3)$$

which is a measure of high mass flux effect.[5] The solid line in the figure represents the numerical correlation under low mass flux conditions (Eq. (2)). The dotted lines represent deviations from the low mass flux correlation[2,12] calculated by the following equation:

$$\frac{Sh(1-\omega_S)}{[Sh(1-\omega_S)]_0} = f_B \cdot g(B_M) \qquad (4)$$

where $g(B_M)$ is the numerical correlation[4] for the effect of high mass flux on a single drop:

$$g(B_M) = \frac{1}{0.3+0.7(1+B_M)^{0.88}} \qquad (5)$$

The figure clearly indicates a systematic decrease in diffusion fluxes with increase of the transfer number for mass transfer, B_M. Good agreement between the data and the single-drop correlation is observed. This may indicate that the effect of high mass flux on co-axially arranged volatile drops may well be predicted by use of Eq. (5).

To confirm this, all the data for evaporation of hexane drops into dry air are plotted against L/D_A in **Fig. 6**. The ordinate is dimensionless diffusion fluxes normalized by those for a single sphere and corrected for the effect of high mass flux with variable properties.* All the data for hexane drops showed good agreement with the low mass flux correlation after due consideration of the effect of high mass flux and of variable physical properties. An explanation for this is that the diffusion fluxes of the rear drop for two coaxially arranged drops are affected by the wake of the front drop but are less affected by the evaporation of the front drop.[11]

3. Final Correlation of the Data

Taking into account the effect of high mass flux by Eq. (5) and of variable properties, all the data for evaporation of water and hexane rear drops into dry air were well correlated by the following equation:

$$\frac{Sh_B(1-\omega_S)}{[Sh(1-\omega_S)]_0}=f_B\cdot g(B_M)\cdot(\rho_\infty/\rho_S)^{1/3} \qquad (6)$$

As was the case for the rear drop, all the data for evaporation of water and hexane front drops into dry air were correlated by the following equations:

$$\frac{Sh_A(1-\omega_S)}{[Sh(1-\omega_S)]_0}=f_A\cdot g(B_M)\cdot(\rho_\infty/\rho_S)^{1/3} \qquad (7)$$

where f_A is the numerical correlation proposed in our previous papers[2,12]:

$$f_A=\frac{1}{1+0.67\cdot(D_B/D_A)^{1.93}\cdot(L/D_A)^{-3.0\cdot Re_{PA}^{0.40}}} \qquad (8)$$

The ranges of variables for the correlation are:

Re_{PA}: 64–230
L/D_A: 0.98–11.04
D_B/D_A: 0.54–1.58
B_M: 0.02–0.64
(ρ_∞/ρ_S): 0.64–0.95

Figure 7 shows a comparison between the observed diffusion fluxes and those calculated by Eq. (6) or (7). Good agreement between the data and the correlation is observed.

* Under high mass flux conditions, variation of physical properties between the free stream and the drop surface due to large temperature differences becomes so large that the assumption of constant physical properties[5] in the theoretical solutions may not hold. Thus the effect of variable physical properties was taken into account for the diffusion fluxes of volatile drops.

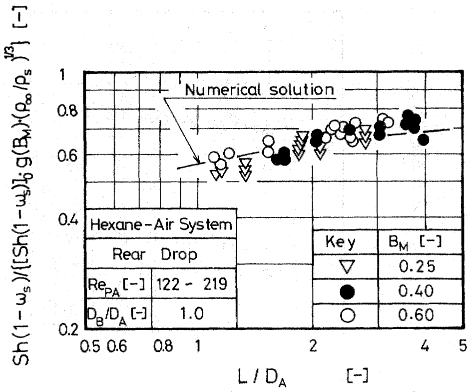

Fig. 6. Effect of distance between two drops on the diffusion fluxes of rear drop; corrected for the effect of high mass flux and of variable properties

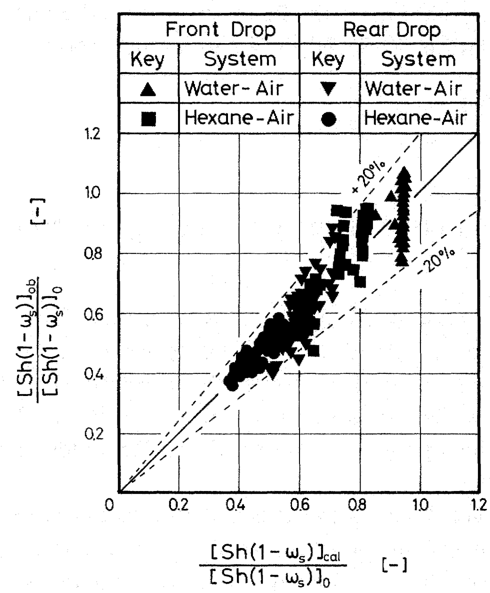

Fig. 7. Comparison of observed data with proposed correlation

Conclusions

Measurements of the rates of evaporation in mass transfer from two coaxially arranged water and hexane drops into a high ambient temperature air stream led to the following conclusions.

1) The observed data showed good agreement with the previous numerical solutions under low mass flux conditions.

2) All the data showed good agreement with the low mass flux correlations (Eqs. (2) and (8)) after due consideration of the effect of high mass flux on a single sphere and of variable physical properties.

Nomenclature

B_M	= transfer number for mass transfer defined by Eq. (3)	[—]
D_A	= diameter of front drop	[m]
D_B	= diameter of rear drop	[m]
D_P	= diameter of drop	[m]

$\mathscr{D}$ = binary diffusion coefficient [m²/s]
f = function of L/D_A, D_B/D_A and Re_{PA} defined by Eqs. (2) and (8) [—]
g = function defined by (5); function of B_M [—]
L = distance between centers of the two drops or spheres [m]
N_A = mass flux of component A [kg/m²·s]
Re_{PA} = Reynolds number ($=D_A U_\infty/\nu_G$) [—]
Sc = Schmidt number ($=\nu_G/\mathscr{D}_G$) [—]
Sh = Sherwood number ($=N_A \cdot D_P/(\rho_S \mathscr{D}_S \omega_S - \omega_\infty)$) [—]
T_∞ = free stream temperature [K]
U_∞ = free stream velocity [m/s]

ν = kinematic viscosity of gas [m²/s]
ρ = density [kg/m³]
ω = mass fraction [—]

⟨Subscripts⟩
A = front drop or sphere
B = rear drop or sphere
cal = calculated value
G = gas phase
ob = observed value
P = drop
S = surface of drop
0 = single sphere
∞ = free stream

Literature Cited

1) Aminzadeh, K., T. R. Al Taha, A. R. H. Cornish, M. S. Kolansky and R. Pfeffer: *Int. J. Heat Mass Transfer*, **17**, 1425 (1974).
2) Asano, K., I. Taniguchi and T. Kawahara: Proceedings of the 4th International Conference on Liquid Atomization and Spray Systems, pp. 411–418 (1988).
3) Brzustowski, T. A., E. M. Twardus, S. Wojcicki and A. Sobiesiak: *AIAA J.*, **17**, 1234 (1979).
4) Chuchottaworn, P., A. Fujinami and K. Asano: *J. Chem. Eng. Japan*, **17**, 1 (1984).
5) Chuchottaworn, P., A. Fujinami and K. Asano: *J. Chem. Eng. Japan*, **17**, 7 (1984).
6) Miura, K., T. Miura and S. Ohtani: *Kagaku Kogaku Ronbunshu*, **1**, 241 (1975).
7) Ranz, W. E. and W. R. Marshall: *Chem. Eng. Progr.*, **48**, 141 (1952).
8) Reid, R. C., J. M. Prausnitz and T. K. Sherwood: "The Properties of Gases and Liquids," 3rd ed., pp. 181–222, 391–601, McGraw-Hill, New York (1977).
9) Rex, J. F., A. E. Fuhs and S. S. Penner: *Jet Propulsion*, **26**, 179 (1956).
10) Tal, R., D. N. Lee and W. A. Sirignano: *Int. J. Heat Mass Transfer*, **27**, 1953 (1984).
11) Taniguchi, I. and K. Asano: *J. Chem. Eng. Japan*, **20**, 287 (1987).
12) Taniguchi, I. and K. Asano: *J. Chem. Eng. Japan*, **22**, 701 (1989).
13) Umemura, A., S. Ogawa and N. Oshima: *Cumbust. Flame*, **41**, 45 (1981).
14) Umemura, A., S. Ogawa and N. Oshima: *Combust. Flame*, **43**, 111 (1981).